

Retinexmamba: Retinex-based Mamba for Low-light Image Enhancement

Jiesong Bai^{1,*}, Yuhao Yin^{1,*}, Qiyuan He¹, Yuanxian Li², and Xiaofeng Zhang^{3,†}

¹ Shanghai University

² Yunnan University

³ Shanghai Jiao Tong University

* Equal contribution. † Corresponding author

Abstract. *In the field of low-light image enhancement, both traditional Retinex methods and advanced deep learning techniques such as Retinexformer have shown distinct advantages and limitations. Traditional Retinex methods, designed to mimic the human eye's perception of brightness and color, decompose images into illumination and reflection components but struggle with noise management and detail preservation under low light conditions. Retinexformer enhances illumination estimation through traditional self-attention mechanisms, but faces challenges with insufficient interpretability and suboptimal enhancement effects. To overcome these limitations, this paper introduces the RetinexMamba architecture. RetinexMamba not only captures the physical intuitiveness of traditional Retinex methods but also integrates the deep learning framework of Retinexformer, leveraging the computational efficiency of State Space Models (SSMs) to enhance processing speed. This architecture features innovative illumination estimators and damage restorer mechanisms that maintain image quality during enhancement. Moreover, RetinexMamba replaces the IG-MSA (Illumination-Guided Multi-Head Attention) in Retinexformer with a Fused-Attention mechanism, improving the model's interpretability. Experimental evaluations on the LOL dataset show that RetinexMamba outperforms existing deep learning approaches based on Retinex theory in both quantitative and qualitative metrics, confirming its effectiveness and superiority in enhancing low-light images. Code is available at <https://github.com/YhuoyuH/RetinexMamba>*

Keywords: Retinex · Low-light Enhancement · Fused-Attention · Retinexformer · State Space Model.

1 Introduction

Low-light enhancement refers to the process of improving the quality and visual appearance of images captured under insufficient light or dim environmental conditions through image processing techniques. This field is of significant importance in computer vision and image processing because images under low-light conditions often suffer from issues such as dimness, blurriness, and unclear details, which affect the quality and usability of the images.

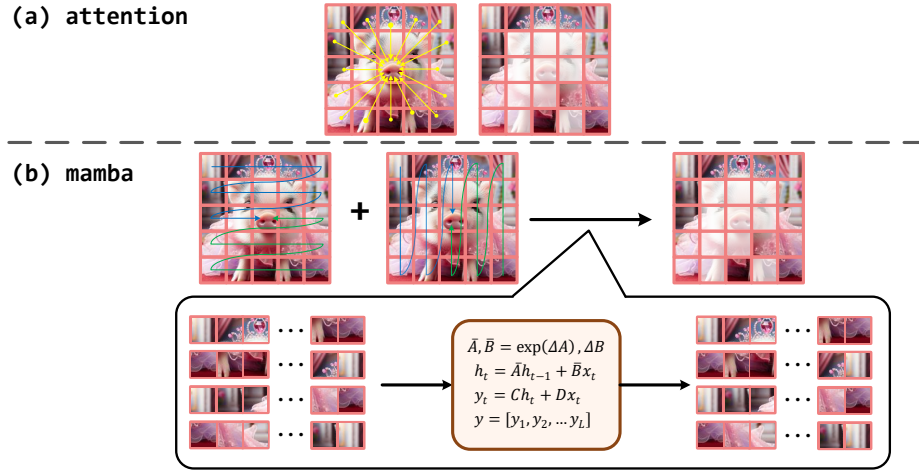


Fig. 1. The image above shows a visual comparison between the attention mechanism and 2D selective scanning in Mamba. In Mamba’s 2D selective scanning, scanning starts simultaneously from all sides of the image, whereas the attention mechanism calculates attention scores separately from the target view to the global view.

Traditional techniques such as histogram equalization[35,34,4,38,1,3,22] and gamma correction[44,18,36], while foundational and important, often fall short in dealing with complex lighting dynamics and maintaining the naturalness of enhanced images. Inspired by the human visual system, the Retinex theory[21] establishes a conceptual framework for separating the illumination and reflection components of an image, paving the way for more sophisticated enhancement strategies capable of addressing diverse and challenging low-light environments.

Recent advancements in neural networks, particularly in the application of Convolutional Neural Networks (CNN) and Transformer models, have set new benchmarks in low-light image enhancement. CNNs[27,42,31,51] exhibit strong capabilities in low-light image enhancement by effectively capturing spatial information and local features within images. However, CNNs may have limitations in modeling long-range dependencies, leading to insufficient consideration of overall image information and challenges in effectively addressing issues like noise amplification and detail preservation in low-light image processing. On the other hand, Transformer models[57,2,54,58,50] achieve global perception and modeling of long-range dependencies through self-attention mechanisms, aiding in more accurately restoring details and structures in images during low-light image processing. However, Transformer models also face challenges such as high computational complexity and large parameter sizes, resulting in potential issues of slow inference speed and high resource consumption in practical applications.

In this context, our work introduces the *RetinexMamba* architecture. Initially following the approach of Retinexformer, we divide the overall architecture into an illumination estimator and a damage repairer. The illumination estimator is used to initially light up the image, while the damage repairer eliminates amplified artifacts and noise generated

during the illumination process, as well as color distortions and overexposure. To address the high computational complexity in Transformers and the insufficient interpretability of the attention mechanism in Retinexformer, the basic unit of our damage repairer is the Illumination Fusion State Space Model (IFSSM). This model utilizes 2D Selective Scanning (SS2D) as the backbone network to achieve linear computational efficiency, and employs Illumination Fusion Attention (IFA) to replace the Illumination-Guided Multi-head Self-Attention (IG-MSA) in Retinexformer to enhance the interpretability of the attention mechanism.

Through comprehensive experimental setups, we provide quantitative and qualitative results that demonstrate the superiority of our model on standard benchmarks such as the LOL dataset[55,49]. According to the data in Tab.1, using this approach, we have surpassed the SOTA of deep learning methods based on Retinex theory on the LOL dataset. Our contributions can be summarized as follows:

1. Introducing Mamba for low-light enhancement for the first time, using SS2D to replace Transformers in capturing long-range dependencies.
2. We proposed a fusion module that better implements the embedding of illumination features consistent with Retinex theory.
3. Extensive quantitative and qualitative experiments prove that our method surpasses all previous deep learning methods based on Retinex theory.

2 Related Work

2.1 Low-light Image Enhancement

Distribution Mapping Method. In early research on low-light image enhancement, one of the most intuitive approaches is to map the distribution of the low-light inputs in a way that amplifies smaller values (which appear dark). Representative techniques of this approach include histogram equalization [35,34,4,38,1,3,22] and S-curve-based methods, such as gamma correction [44,18,36]. However, existing distribution mapping-based methods often suffer from color distortion and other artifacts that affect the visual quality of the enhancement results, due to the lack of recognition and utilization of semantic information during the distribution mapping process.

Traditional Model Method. Retinex theory [21] provides an intuitive physical explanation for the process of enhancing weakly lit images. This theory postulates that desired normal images (i.e., reflectance maps) can be obtained by removing the illumination component from low-light inputs. Jobson et al.[19,20] conducted exploratory research based on the Retinex model. As research progressed, it became apparent that the key to achieving brightness enhancement using the Retinex approach is the estimation of the illumination layer [37,43,7,6,14]. Such methods rely on manually crafted priors and often require careful parameter tuning. Inaccurate priors or regularization can result in artefacts and color bias in the enhanced images, demonstrating poor generalization capabilities and a time-consuming optimization process. Additionally, these studies often overlook the presence of noise, which can result in its retention or amplification in the enhanced images.

Deep Learning Method. Deep learning-based methods for low-light image enhancement originated in 2017 [26] and subsequently became the leading approach in the field. Following the traditional Retinex theory [21] as a cornerstone for model architecture, a series of works were designed along these lines [46,24]. CNN [27,42,31,51,40,47,52,30] has been widely used in low-light image enhancement. For example, Wei et al. [45] and subsequent works [55,56] combined Retinex decomposition with deep learning. However, these CNN-based methods had limitations in capturing long-range dependencies across different regions. Star [57] introduced the transformer architecture to the field of low-light enhancement, addressing the issue of capturing long-range dependencies. Meanwhile, Retinexformer [2] combined the Retinex theory with the design of a one-stage transformer, further refining and optimizing this approach. Nonetheless, transformer models pose significant computational burdens and complexity when dealing with long sequences due to their self-attention mechanisms.

2.2 State Space models

Recently, the state space models (SSMs) have been increasingly recognized as a promising direction in research. A structured state space sequence model, referred to as S4, was proposed in [12] as a novel alternative to CNNs or Transformers for modeling long-range dependencies. Subsequent developments have seen various structured state space models emerge, featuring complex diagonals [15,11], multi-input multi-output support [41], diagonal decomposition and low-rank operations [16] enhancing their expressive capabilities. Contemporary SSMs such as Mamba [10] not only establish long-distance dependency relations but also demonstrate linear complexity with respect to input size. Models based on SSM architecture have garnered extensive research interest across diverse domains [33]. The selective scanning mechanism introduced by Mamba [10] matches the performance of prevalent foundational models in vision, such as [17,5,25]. Vision Mamba [60] suggests that pure SSM models can serve as a generic visual backbone. Empirical validation is provided by [39,28], which have shown promise in the task of medical image segmentation, while in low-level vision tasks, applications such as [59,9] have demonstrated favorable outcomes. Inspired by this research, our work leverages Mamba’s capability for linear analysis of long-distance sequences to process features fused with Retinex theory [21]. The resulting enhancements to low-light images substantiate the potential of Mamba-based models in the domain of low-light image enhancement.

3 Method

Fig. 2 depicts the comprehensive structure of our approach. As illustrated in Fig. 2, our RetinexMamba consists of an Illumination Estimator (a) and a Damage Restorer (b). The Illumination Estimator (IE) is influenced by the conventional Retinex theory. The design of the Damage Restorer is based on the Illumination Fusion Visual Mamba (IFVM). Displayed in Fig. 2(b), the core component of IFVM is the Illumination Fusion State Space Model (IFSSM), featuring a Layer Normalization (LN), an Illumination-Fused Attention Mechanism (IFA), a 2D Selective Scan(SS2D), and a Feed-Forward Network (FFN). The specifics of the IFA are detailed in Figure 2(c).

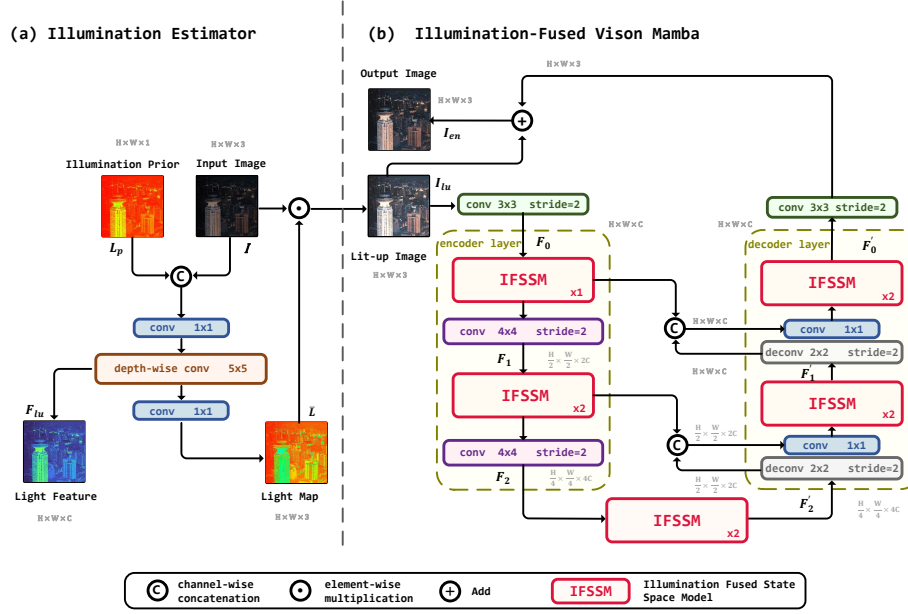


Fig. 2. Our structural framework is displayed in the two main areas above. It comprises an illumination estimator (a) and a Damage Restorer based on the Illumination Fusion Visual Mamba (IFVM) (b).

3.1 Retinex-based Framework

The traditional Retinex image enhancement algorithm simulates human visual perception of brightness and color. It decomposes image $I \in \mathbb{R}^{H \times W \times 3}$ into the illumination component $L \in \mathbb{R}^{H \times W}$ and the reflection component $R \in \mathbb{R}^{H \times W \times 3}$. This conclusion can be expressed by the following formula:

$$I = R \circ L \quad (1)$$

where \circ denotes element-wise multiplication. The reflection component R is determined by the intrinsic properties of the object, while the illumination component L represents the lighting conditions. However, under this formulaic expression, the traditional Retinex algorithm does not account for the noise and artifacts produced by unbalanced light distribution or dark scenes in low-light conditions, and this loss of quality is further amplified with the enhancement of the image. Therefore, inspired by the Retinex algorithm, we have adopted the perturbation modeling proposed by [2], which introduces perturbation terms for the illumination and reflection components \tilde{L} and \tilde{R} in the original formula, as shown in the following equation:

$$I = (R + \tilde{R}) \circ (L + \tilde{L}) \quad (2)$$

$$= R \circ L + R \circ \tilde{L} + \tilde{R} \circ L + \tilde{R} \circ \tilde{L}, \quad (3)$$

where $\tilde{R} \in \mathbb{R}^{H \times W \times 3}$ and $\tilde{L} \in \mathbb{R}^{H \times W}$ represent the perturbation terms for the reflection and illumination components respectively. After simplification, we can express the illuminated image I_{lu} as follows:

$$I_{lu} = I \circ \bar{L} = R + C, \quad (4)$$

where \bar{L} represents the illumination mapping, which is obtained through convolution for feature extraction, and $C \in \mathbb{R}^{H \times W \times 3}$ denotes all the losses previously mentioned. Hence, our RetinexMamba can be expressed as:

$$(I_{lu}, F_{lu}) = IE(I, L_p), \quad (5)$$

$$I_{en} = IFVM(I_{lu}, F_{lu}), \quad (6)$$

$$RM = IE(I_{lu}, L_p) + IFVM(I_{lu}, F_{lu}), \quad (7)$$

where IE represents the Illumination Estimator, and IFVM denotes the Damage Restorer. IE takes the low-light image I and the illumination prior $L_p \in \mathbb{R}^{H \times W}$ as input, outputting the illuminated image $I_{lu} \in \mathbb{R}^{H \times W \times 3}$ and the illumination feature map $F_{lu} \in \mathbb{R}^{H \times W \times C}$. The L_p is obtained by calculating the average value of each channel of the image, used to assess the overall brightness or illumination level of the image; hence we use L_p as an illumination prior to provide lighting information for the image. Then, these two results are fed into the Damage Restorer (IFVM) to mend the quality loss amplified during the illumination of the image, and finally generate the repaired result $I_{en} \in \mathbb{R}^{H \times W \times 3}$.

Illumination Estimator. The structure of the Illumination Estimator(IE) is shown in Fig. 2(a). We merge the low-light original image I with the illumination prior L_p obtained through calculation, and increase the channel dimension to serve as input. This is followed by three convolutions to extract features. The first *conv* 1×1 merges the previously combined input, that is, to apply the illumination prior to the fusion into the low-light image. The second depthwise separable *conv* 5×5 upsamples the input, further extracting features to generate the illumination feature map F_{lu} , where the feature dimension n_{feat} is set to 40. Finally, another *conv* 1×1 is used for downsampling to recover the 3-channel illumination mapping \bar{L} , which is then element-wise multiplied by the low-light image I to obtain the illuminated image I_{lu} .

Illumination-Fused Vision Mamba. The structure of the Damage Restorer (IFVM) is shown in Fig. 2(b), which consists of an encoder and a decoder based on the illumination fusion visual mamba. The encoder represents the downsampling process, while the decoder represents the upsampling process. The upsampling and downsampling processes are symmetric and divided into two levels. Firstly, the illuminated image I_{lu} obtained from the Illumination Estimator IE is downsampled by a *conv* 3×3 (stride = 2) to match the dimension of the illumination feature map F_{lu} , facilitating subsequent operations. Next, we perform downsampling to reduce computational complexity and extract deep features. The downsampling process is divided into two levels, each level consisting of an Illumination Fusion State Space Model (IFSSM) and a convolutional layer with a stride of 2 and kernel size of 4×4 . After each convolutional layer, the width and height of the

image are halved, while the feature dimension is doubled. Therefore, after two levels of downsampling, the deepest feature dimension should be $4C$. After extracting image features, we need to perform upsampling to recover the image. Similar to downsampling, upsampling is also divided into two levels, each consisting of a *deconv* 2×2 (stride = 2) and a *conv* 1×1 , and an Illumination Fusion State Space Model (IFSSM). After each deconvolution layer, the width and height of the image are doubled, while the feature dimension is halved. The output of the deconvolution layers is then linked with the corresponding level of downsampling Illumination Fusion State Space Model (IFSSM) output to mitigate the loss of image information during downsampling. Finally, a *conv* 3×3 (stride = 2) is applied to the image to reduce the dimensionality and restore it to the RGB format with three channels. The enhanced image I_{en} is obtained by performing a residual connection with the restored image and I_{lu} .

3.2 Illumination-Fused State Space Models.

In low-light enhancement research, Convolutional Neural Networks (CNNs) have limitations in processing overall image information. Transformers may affect the efficiency of practical applications due to their high computational demands. To address this, our designed Illumination Fusion State Space Model (IFSSM) includes Fused Attention (IFA), an SS2D module, an LN layer, a Feed-Forward Network (FFN), and a convolutional layer to match the dimensions of illumination feature maps with inputs, as shown in Fig. 3.

Illumination-Fused Attention. As shown in Fig.3, the illumination feature map F_{lu} generated by IE is input together with the brightened image after feature extraction into IFA. In [2], the illumination feature map F_{lu} is used as a token, transformed and multiplied with V (value) generated from x to calculate attention scores. However, this method results in KV (key and value) not coming from the same input, violating the principle in Transformers of ensuring that all information processing focuses on the content of the input data rather than external or irrelevant information to the current task, breaking data consistency and alignment, and the additional multiplication operation also increases parameter requirements and computational complexity. Therefore, our IFA adopts the Cross Attention mechanism, first adjusting F_{lu} and input x to a form suitable for multi-head attention by changing dimensions:

$$\mathbf{X} = [X_1, X_2, \dots, X_k], \quad \mathbf{F}_{lu} = [F_{lu1}, F_{lu2}, \dots, F_{luk}] \quad (8)$$

where $X_i \in \mathbb{R}^{HW \times d_k}$, $F_{lui} \in \mathbb{R}^{HW \times d_k}$, k is the number of heads, d_k denotes the dimensionality of each head, and $d_k = \frac{C}{k}$, with C representing the dimensionality of the input features. We note that using an illumination prior map as the query vector allows the model to more specifically address the dark areas in the image. Consequently, the attention mechanism of the model can focus on the low-light areas that need enhancement, rather than processing the entire image uniformly. Therefore, we treat F_{lu} as $Q \in \mathbb{R}^{HW \times d_k}$ and the input x as $K, V \in \mathbb{R}^{HW \times d_k}$, to fuse the two input features, enabling F_{lu} to guide the self-attention calculation of x .

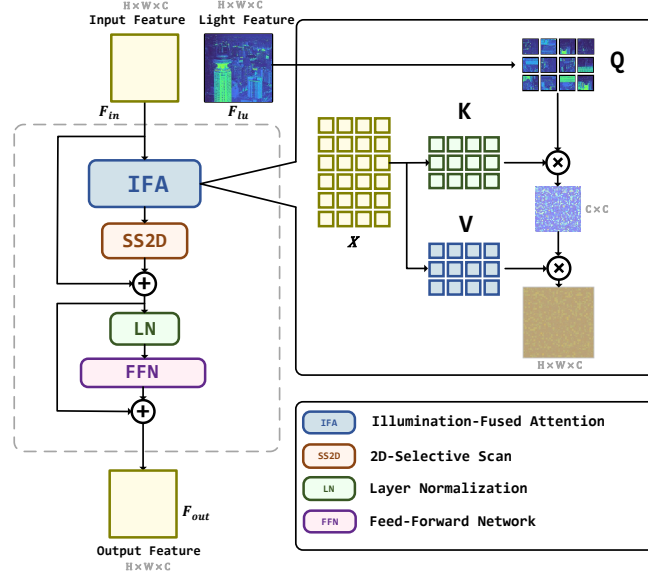


Fig. 3. Our Illumination Fusion State Space Model (IFSSM) integrates lighting features and input vector x using a fused-block, and utilizes the linear 2D Selective Scanning model (SS2D) for feature extraction. In IFA, we treat lighting features as Q , and input vectors as KV to calculate attention scores.

$$Q_i = \mathbf{F}_{lu_i} W_{Q_i}, \quad K_i = X_i W_{K_i}, \quad V_i = X_i W_{V_i}, \quad (9)$$

where W_Q, W_K , and $W_V \in \mathbb{R}^{d_k \times d_k}$ are the learnable parameter matrices constructed by convolutional layers. Thus, the self-attention of each head can be represented by the formula:

$$\text{Attention}(Q_i, K_i, V_i) = (V_i) \text{softmax} \left(\frac{K_i^T Q_i}{\alpha_i} \right), \quad (10)$$

where $\alpha_i \in \mathbb{R}^1$ is a learnable parameter serving as a scaling factor to adjust the attention scores, thereby controlling the sharpness of the attention weights, the k heads are subsequently reshaped back to the standard image format (B, C, H, W) and aggregated via a convolutional layer, resulting in an output with dimensions that match the original.

2D-Selective Scan. Inspired by the SSM model in [10], we adopted the approach of integrating an SSM into visual tasks from [47]. The SS2D module in [47] consists of Scan Expanding, S6 blocks, and Scan Merging operations. For the processed images we input, they first undergo the Scan Expanding operation, where the image is unfolded from its four corners as shown in Fig. 1. The images are then flattened, meaning the height (H) and width (W) are merged into a token length (L). Each sequence from the

scan is then input into an S6 module for feature extraction. The calculation formula for S6 can be expressed as:

$$h_t = \bar{A}h_{t-1} + \bar{B}x_t \quad (11)$$

$$y_t = \bar{C}h_t \quad (12)$$

where x is the input variable, y is the output, and \bar{A}, \bar{B} and \bar{C} are all learnable parameters. Afterward, the outputs from the four directions of extracted features y_1, y_2, y_3, y_4 are summed and merged, and the dimensions of the merged output are readjusted to match the input size. Furthermore, to extract deeper latent features, we set the number of hidden layers in SS2D to increase with each level of IFSSM. We default the number of hidden layers d_{state} in SS2D to 16, doubling the number of layers with each sampling level, thus reaching up to 64 layers at the deepest sampling. This setting allows for progressively deeper feature extraction from the vector that has integrated illumination features.

4 Experiment

4.1 Datasets and Implementation details

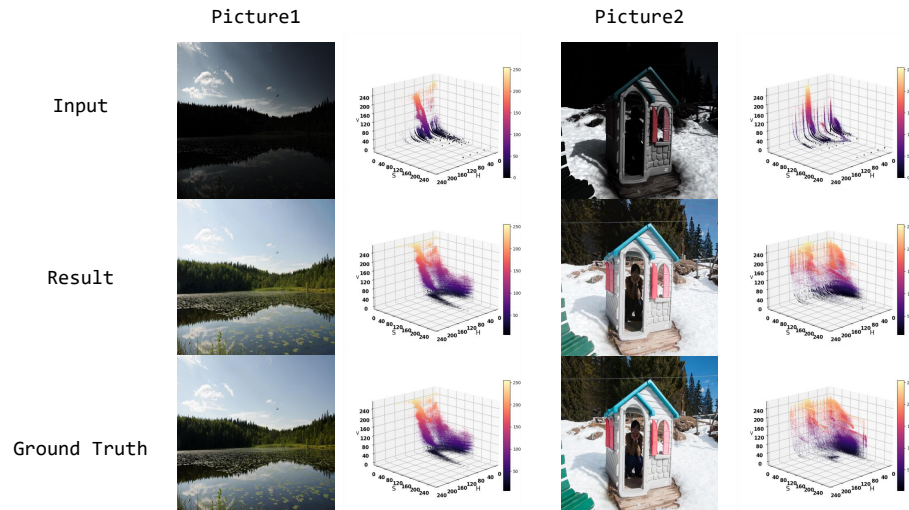


Fig. 4. 3D image display of the HSV color space.

We evaluated the performance of our model on the LOL dataset (v1[55] and v2[49]).

LOL. The LOL dataset is divided into two versions, v1 and v2. In LOL_v1, the ratio of training to test data pairs is 485:15. Each pair consists of an input low-light image

and a target reference image. The LOL_v2 dataset is further divided into LOLv2_real and LOLv2_synthetic. The ratios of training to test data pairs in LOLv2_real and LOLv2_synthetic are 689:100 and 900:100, respectively. The distribution of data pairs is the same as in LOL_v1.

Implementation Details. We implemented our RetinexMamba model in Pytorch and trained and tested it on a PC with A10 and V100 GPUs under a Linux system (CUDA 11.7, Python 3.8, Pytorch 1.13). We set the resolution of images to 128x128. The batch sizes for LOL_v1 and LOLv2-synthetic were set to 8, and for LOLv2_real to 4. Standard augmentation methods such as random rotation and flipping were used to enhance the training data. To minimize loss, we employed the Adam optimizer with a momentum term β_1 set at 0.9 and RMSprop control parameter β_2 set at 0.999, aiming to minimize the Mean Absolute Error (MAE) between the enhanced images and the ground truth. Additionally, a cosine annealing schedule was used to prevent the loss from getting stuck in local minima.

Table 1. Quantitative comparisons on LOL-v1 and LOLv2-real

Methods	LOL-v1			LOLv2-real		
	PSNR \uparrow	SSIM \uparrow	RMSE \downarrow	PSNR \uparrow	SSIM \uparrow	RMSE \downarrow
Supervised						
LIME[14]	16.362	0.624	21.07	16.342	0.653	22.54
MBLEN[27]	17.938	0.699	18.78	15.950	0.701	30.22
Retinex-Net[45]	17.188	0.589	22.59	16.410	0.640	20.21
KinD[56]	20.347	0.813	14.30	18.070	0.781	18.04
KinD++[55]	20.707	0.791	14.34	16.800	0.741	15.64
MIRNet [51]	24.140	0.842	12.03	20.357	0.782	14.21
URetinex-Net[46]	21.450	0.795	13.55	21.554	0.801	14.23
Retinexformer[2]	23.932	0.831	8.35	21.230	0.838	9.92
RetinexMamba	24.025	0.827	8.17	22.453	0.844	9.38
Unsupervised						
GenerativePrior [32]	12.552	0.410	45.80	13.041	0.552	40.23
Zero-Dce [13]	16.760	0.560	34.42	18.059	0.580	29.01
RUAS [24]	16.401	0.503	30.21	16.873	0.513	29.23
SCI [29]	14.864	0.542	24.87	15.342	0.521	27.50
PairLie [8]	19.691	0.712	19.03	19.288	0.684	20.01
NeRCO [48]	19.701	0.771	24.80	19.234	0.671	23.13
CLIP-LIE [23]	17.207	0.589	10.18	17.057	0.589	10.64
Enlighten-Your-Voice [53]	19.728	0.715	10.13	19.335	0.686	10.21

4.2 Low-light Image Enhancement

We compare our method against various SOTA methods in both supervised and unsupervised domains in Tab.1. The datasets used for comparison are the synthetic data from LOLv1 and the real data from LOLv2. All data in the table were obtained under the same conditions using publicly available code for training and testing or derived from the original papers. The results indicate that our method outperforms the aforementioned SOTAs in terms of PSNR and RMSE, while SSIM is slightly lower than that of Retinexformer.

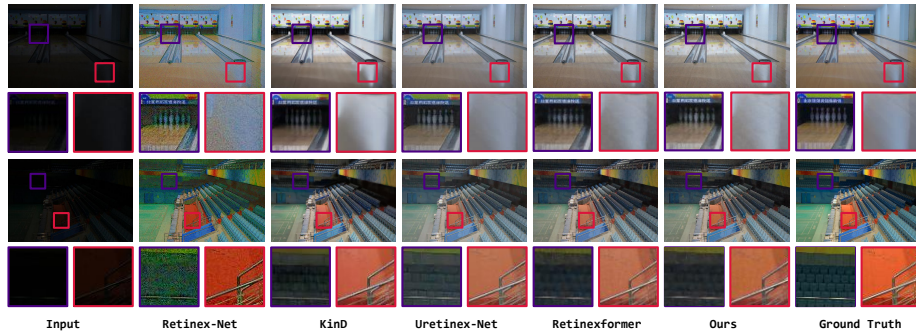


Fig. 5. The above are the qualitative experimental results on LOLv1. Our method effectively reduced color distortion and enhanced the lighting effects.

Quantitative Results. The metrics we used for comparison include PSNR, SSIM, and RMSE. A higher PSNR indicates better image enhancement effects, while a higher SSIM indicates the preservation of more high-frequency details and structures in the results. A lower RMSE value signifies better performance of the prediction model, as it indicates smaller errors. Compared to the baseline and the best existing technology method[2], our method achieved an increase in PSNR by 0.093 and 0.77 on the LOL_v1 and LOLv2_real datasets, respectively. RMSE decreased by 0.39 on the LOLv2_real dataset, which is desirable as lower values are better.

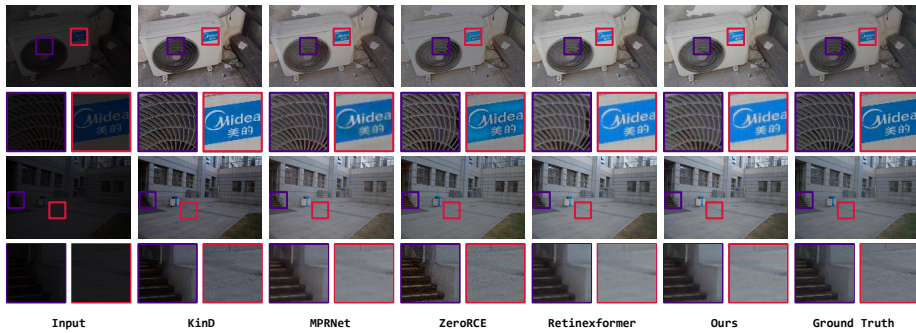


Fig. 6. The above are the qualitative experimental results on LOLv1. Our method effectively reduced color distortion and enhanced the lighting effects.

Qualitative Results. The qualitative comparison results between RetinexMamba and other SOTA algorithms are shown in Fig. 5 and 6. Please zoom in for better visual clarity. Figure Three compares the LOLv1 dataset, while Fig. 6 compares the LOLv2_real dataset. As depicted in Figure Three, previous methods exhibit amplification of noise,

such as in Retinex-Net, as well as cases of underexposure like KinD and overexposure like Uretinex-Net. Similarly, on the synthetic dataset in Fig. 6, KinD shows instances of overexposure in the air conditioner area at the top and underexposure in the staircase area at the bottom, while ZeroRCE exhibits extensive noise and artifacts. Likewise, in Retinexformer, underexposure around the bowling ball at the top of Fig. 5 and color distortion in the stadium at the bottom are observed. In contrast, our RetinexMamba effectively controls exposure intensity, reduces color distortion, and minimizes noise. Additionally, we compared two images on the LOLv2_syn dataset in both 2D and 3D HSV color space in Figs. 7 and 4. The results demonstrate that the images enhanced by RetinexMamba are closest to the Ground Truth.

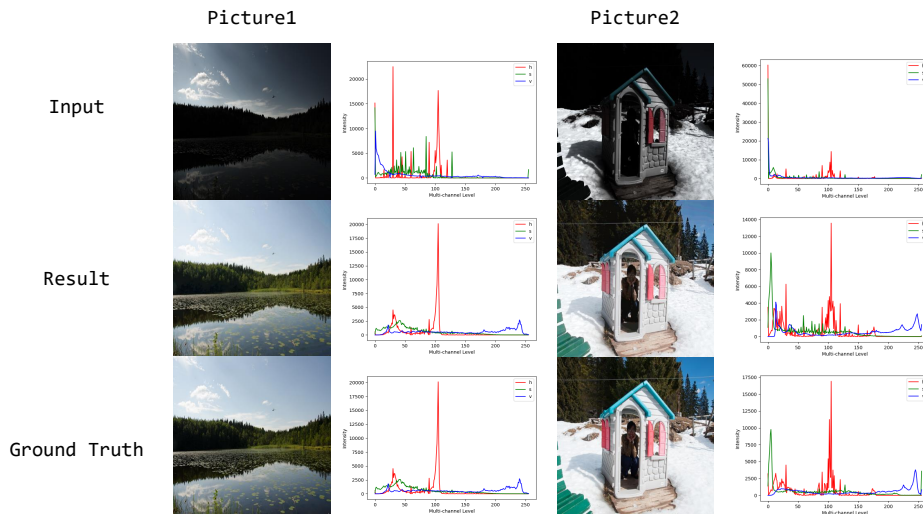


Fig. 7. 2D image display of the HSV color space.

4.3 Ablation Study

Table 2. Ablation Study on LOL-v1, LOLv2-real and LOLv2-syn

Methods	LOL-v1			LOLv2-real			LOLv2-syn		
	PSNR \uparrow	SSIM \uparrow	RMSE \downarrow	PSNR \uparrow	SSIM \uparrow	RMSE \downarrow	PSNR \uparrow	SSIM \uparrow	RMSE \downarrow
Ours FixedHS	23.839	0.823	8.29	21.756	0.832	9.51	25.419	0.928	8.34
Ours NoFB	22.730	0.826	8.70	22.262	0.823	9.27	25.343	0.934	8.40
Ours NoSS2D	23.035	0.821	8.75	21.309	0.807	9.74	24.861	0.923	8.43
Ours IGMSA	22.054	0.797	9.51	21.745	0.824	9.46	25.236	0.928	8.43
RetinexMamba	24.025	0.827	8.17	22.453	0.844	9.38	25.887	0.935	8.24

We conduct our ablation studies on three datasets: LOLv1, LOLv2_real, and LOLv2_syn. We have set up six different architectures here, each varying by removing different components or setting different hyperparameters for comparison.

- "Ours FixedHS" denotes that we have set the number of hidden layers d_{state} in the SS2D module of IFSSM to a fixed value of 16, which no longer deepens as the sampling levels increase.
- "Ours NoFB" indicates that we have removed the fused-block in IFSSM and used element-wise multiplication to fuse the illumination features and the input vector.
- "Ours NoSS2D" indicates that we have removed the SS2D module from IFSSM, retaining only the Transformer architecture.
- "Ours IGMSA" denotes that we have replaced the fused attention in IFSSM with the Illumination-Guided Multi-head Self-Attention (IG-MSA) from [2].

Compared to all ablation results, our ablation setup achieved the highest PSNR and SSIM. "Ours FixedHS" demonstrated the drawbacks of insufficient feature extraction and the inability to capture long sequences with a fixed number of hidden layers in the SS2D model. "Ours NoFB", which uses direct element-wise multiplication to fuse illumination features, lacks a logical explanation. Meanwhile, "Ours NoSS2D" and "Ours IGMSA" each highlight the disadvantages of using only the Transformer architecture and the poor interpretability of attention calculations from [2], respectively.

5 Conclusion

In this paper, we introduce the RetinexMamba architecture, which is based on the Retinexformer and Mamba to enhance low-light images. Initially, building on the Retinexformer model, we divided it into an illumination estimator and a damage restorer, and inspired by VMamba, we incorporated the SS2D model to address the inherent position sensitivity of visual data in Transformers. Furthermore, we replaced the IG-MSA module with a more interpretable Fused-Attention to fuse illumination features and the input vector. Extensive quantitative and qualitative experiments demonstrate that our RetinexMamba outperforms the current state-of-the-art on the LOL dataset. Although the computational complexity of SS2D is reduced, the overall number of parameters has increased, consuming more computational resources. Therefore, our future work will focus on reducing the total number of parameters while maintaining computational complexity.

References

1. Abdullah-Al-Wadud, M., Kabir, M.H., Dewan, M.A.A., Chae, O.: A dynamic histogram equalization for image contrast enhancement. *IEEE transactions on consumer electronics* **53**(2), 593–600 (2007)
2. Cai, Y., Bian, H., Lin, J., Wang, H., Timofte, R., Zhang, Y.: Retinexformer: One-stage retinex-based transformer for low-light image enhancement. In: *Proceedings of the IEEE/CVF International Conference on Computer Vision*. pp. 12504–12513 (2023)

3. Celik, T., Tjahjadi, T.: Contextual and variational contrast enhancement. *IEEE Transactions on Image Processing* **20**(12), 3431–3441 (2011)
4. Cheng, H.D., Shi, X.: A simple and effective histogram equalization approach to image enhancement. *Digital signal processing* **14**(2), 158–170 (2004)
5. Dosovitskiy, A., Beyer, L., Kolesnikov, A., Weissenborn, D., Zhai, X., Unterthiner, T., Dehghani, M., Minderer, M., Heigold, G., Gelly, S., et al.: An image is worth 16x16 words: Transformers for image recognition at scale. *arXiv preprint arXiv:2010.11929* (2020)
6. Fu, X., Zeng, D., Huang, Y., Liao, Y., Ding, X., Paisley, J.: A fusion-based enhancing method for weakly illuminated images. *Signal Processing* **129**, 82–96 (2016)
7. Fu, X., Zeng, D., Huang, Y., Zhang, X.P., Ding, X.: A weighted variational model for simultaneous reflectance and illumination estimation. In: *Proceedings of the IEEE conference on computer vision and pattern recognition*. pp. 2782–2790 (2016)
8. Fu, Z., Yang, Y., Tu, X., Huang, Y., Ding, X., Ma, K.K.: Learning a simple low-light image enhancer from paired low-light instances. In: *Proceedings of the IEEE/CVF conference on computer vision and pattern recognition*. pp. 22252–22261 (2023)
9. Gao, H., Dang, D.: Aggregating local and global features via selective state spaces model for efficient image deblurring. *arXiv preprint arXiv:2403.20106* (2024)
10. Gu, A., Dao, T.: Mamba: Linear-time sequence modeling with selective state spaces. *arXiv preprint arXiv:2312.00752* (2023)
11. Gu, A., Goel, K., Gupta, A., Ré, C.: On the parameterization and initialization of diagonal state space models. *Advances in Neural Information Processing Systems* **35**, 35971–35983 (2022)
12. Gu, A., Goel, K., Ré, C.: Efficiently modeling long sequences with structured state spaces. *arXiv preprint arXiv:2111.00396* (2021)
13. Guo, C., Li, C., Guo, J., Loy, C.C., Hou, J., Kwong, S., Cong, R.: Zero-reference deep curve estimation for low-light image enhancement. In: *Proceedings of the IEEE/CVF conference on computer vision and pattern recognition*. pp. 1780–1789 (2020)
14. Guo, X., Li, Y., Ling, H.: Lime: Low-light image enhancement via illumination map estimation. *IEEE Transactions on image processing* **26**(2), 982–993 (2016)
15. Gupta, A., Gu, A., Berant, J.: Diagonal state spaces are as effective as structured state spaces. *Advances in Neural Information Processing Systems* **35**, 22982–22994 (2022)
16. Hasani, R., Lechner, M., Wang, T.H., Chahine, M., Amini, A., Rus, D.: Liquid structural state-space models. *arXiv preprint arXiv:2209.12951* (2022)
17. He, K., Zhang, X., Ren, S., Sun, J.: Deep residual learning for image recognition. In: *Proceedings of the IEEE conference on computer vision and pattern recognition*. pp. 770–778 (2016)
18. Huang, S.C., Cheng, F.C., Chiu, Y.S.: Efficient contrast enhancement using adaptive gamma correction with weighting distribution. *IEEE transactions on image processing* **22**(3), 1032–1041 (2012)
19. Jobson, D.J., Rahman, Z.u., Woodell, G.A.: A multiscale retinex for bridging the gap between color images and the human observation of scenes. *IEEE Transactions on Image processing* **6**(7), 965–976 (1997)
20. Jobson, D.J., Rahman, Z.u., Woodell, G.A.: Properties and performance of a center/surround retinex. *IEEE transactions on image processing* **6**(3), 451–462 (1997)
21. Land, E.H., McCann, J.J.: Lightness and retinex theory. *Josa* **61**(1), 1–11 (1971)
22. Lee, C., Lee, C., Kim, C.S.: Contrast enhancement based on layered difference representation of 2d histograms. *IEEE transactions on image processing* **22**(12), 5372–5384 (2013)
23. Liang, Z., Li, C., Zhou, S., Feng, R., Loy, C.C.: Iterative prompt learning for unsupervised backlit image enhancement. In: *Proceedings of the IEEE/CVF International Conference on Computer Vision*. pp. 8094–8103 (2023)

24. Liu, R., Ma, L., Zhang, J., Fan, X., Luo, Z.: Retinex-inspired unrolling with cooperative prior architecture search for low-light image enhancement. In: Proceedings of the IEEE/CVF conference on computer vision and pattern recognition. pp. 10561–10570 (2021)
25. Liu, Z., Hu, H., Lin, Y., Yao, Z., Xie, Z., Wei, Y., Ning, J., Cao, Y., Zhang, Z., Dong, L., et al.: Swin transformer v2: Scaling up capacity and resolution. In: Proceedings of the IEEE/CVF conference on computer vision and pattern recognition. pp. 12009–12019 (2022)
26. Lore, K.G., Akintayo, A., Sarkar, S.: Llnet: A deep autoencoder approach to natural low-light image enhancement. *Pattern Recognition* **61**, 650–662 (2017)
27. Lv, F., Lu, F., Wu, J., Lim, C.: Mblen: Low-light image/video enhancement using cnns. In: BMVC. vol. 220, p. 4. Northumbria University (2018)
28. Ma, J., Li, F., Wang, B.: U-mamba: Enhancing long-range dependency for biomedical image segmentation. arXiv preprint arXiv:2401.04722 (2024)
29. Ma, L., Ma, T., Liu, R., Fan, X., Luo, Z.: Toward fast, flexible, and robust low-light image enhancement (2022)
30. Mei, X., Ye, X., Zhang, X., Liu, Y., Wang, J., Hou, J., Wang, X.: Uir-net: A simple and effective baseline for underwater image restoration and enhancement. *Remote Sensing* **15**(1), 39 (2022)
31. Moran, S., Marza, P., McDonagh, S., Parisot, S., Slabaugh, G.: Deeplpf: Deep local parametric filters for image enhancement. In: Proceedings of the IEEE/CVF conference on computer vision and pattern recognition. pp. 12826–12835 (2020)
32. Pan, X., Zhan, X., Dai, B., Lin, D., Loy, C.C., Luo, P.: Exploiting deep generative prior for versatile image restoration and manipulation. *IEEE Transactions on Pattern Analysis and Machine Intelligence* **44**(11), 7474–7489 (2021)
33. Patro, B.N., Agneeswaran, V.S.: Mamba-360: Survey of state space models as transformer alternative for long sequence modelling: Methods, applications, and challenges. arXiv preprint arXiv:2404.16112 (2024)
34. Pisano, E.D., Zong, S., Hemminger, B.M., DeLuca, M., Johnston, R.E., Muller, K., Braeuning, M.P., Pizer, S.M.: Contrast limited adaptive histogram equalization image processing to improve the detection of simulated spiculations in dense mammograms. *Journal of Digital Imaging* **11**, 193–200 (1998)
35. Pizer, S.M., Amburn, E.P., Austin, J.D., Cromartie, R., Geselowitz, A., Greer, T., ter Haar Romeny, B., Zimmerman, J.B., Zuiderveld, K.: Adaptive histogram equalization and its variations. *Computer vision, graphics, and image processing* **39**(3), 355–368 (1987)
36. Rahman, S., Rahman, M.M., Abdullah-Al-Wadud, M., Al-Quaderi, G.D., Shoyaib, M.: An adaptive gamma correction for image enhancement. *EURASIP Journal on Image and Video Processing* **2016**, 1–13 (2016)
37. Rahman, Z.u., Jobson, D.J., Woodell, G.A.: Retinex processing for automatic image enhancement. *Journal of Electronic imaging* **13**(1), 100–110 (2004)
38. Reza, A.M.: Realization of the contrast limited adaptive histogram equalization (clahe) for real-time image enhancement. *Journal of VLSI signal processing systems for signal, image and video technology* **38**, 35–44 (2004)
39. Ruan, J., Xiang, S.: Vm-unet: Vision mamba unet for medical image segmentation. arXiv preprint arXiv:2402.02491 (2024)
40. Sharma, A., Tan, R.T.: Nighttime visibility enhancement by increasing the dynamic range and suppression of light effects. In: Proceedings of the IEEE/CVF Conference on Computer Vision and Pattern Recognition. pp. 11977–11986 (2021)
41. Smith, J.T., Warrington, A., Linderman, S.W.: Simplified state space layers for sequence modeling. arXiv preprint arXiv:2208.04933 (2022)
42. Wang, R., Zhang, Q., Fu, C.W., Shen, X., Zheng, W.S., Jia, J.: Underexposed photo enhancement using deep illumination estimation. In: Proceedings of the IEEE/CVF conference on computer vision and pattern recognition. pp. 6849–6857 (2019)

43. Wang, S., Zheng, J., Hu, H.M., Li, B.: Naturalness preserved enhancement algorithm for non-uniform illumination images. *IEEE transactions on image processing* **22**(9), 3538–3548 (2013)
44. Wang, Z.G., Liang, Z.H., Liu, C.L.: A real-time image processor with combining dynamic contrast ratio enhancement and inverse gamma correction for pdp. *Displays* **30**(3), 133–139 (2009)
45. Wei, C., Wang, W., Yang, W., Liu, J.: Deep retinex decomposition for low-light enhancement. *arXiv preprint arXiv:1808.04560* (2018)
46. Wu, W., Weng, J., Zhang, P., Wang, X., Yang, W., Jiang, J.: Uretinex-net: Retinex-based deep unfolding network for low-light image enhancement. In: *Proceedings of the IEEE/CVF conference on computer vision and pattern recognition*. pp. 5901–5910 (2022)
47. Xu, X., Wang, R., Fu, C.W., Jia, J.: Snr-aware low-light image enhancement. In: *Proceedings of the IEEE/CVF conference on computer vision and pattern recognition*. pp. 17714–17724 (2022)
48. Yang, S., Ding, M., Wu, Y., Li, Z., Zhang, J.: Implicit neural representation for cooperative low-light image enhancement. In: *Proceedings of the IEEE/CVF International Conference on Computer Vision*. pp. 12918–12927 (2023)
49. Yang, W., Wang, W., Huang, H., Wang, S., Liu, J.: Sparse gradient regularized deep retinex network for robust low-light image enhancement. *IEEE Transactions on Image Processing* **30**, 2072–2086 (2021)
50. Yao, J., Wu, T., Zhang, X.: Improving depth gradient continuity in transformers: A comparative study on monocular depth estimation with cnn. *arXiv preprint arXiv:2308.08333* (2023)
51. Zamir, S.W., Arora, A., Khan, S., Hayat, M., Khan, F.S., Yang, M.H., Shao, L.: Learning enriched features for real image restoration and enhancement. In: *Computer Vision–ECCV 2020: 16th European Conference, Glasgow, UK, August 23–28, 2020, Proceedings, Part XXV* 16. pp. 492–511. Springer (2020)
52. Zhang, X., Chen, F., Wang, C., Tao, M., Jiang, G.P.: Sienet: Siamese expansion network for image extrapolation. *IEEE Signal Processing Letters* **27**, 1590–1594 (2020)
53. Zhang, X., Xu, Z., Tang, H., Gu, C., Chen, W., Zhu, S., Guan, X.: Enlighten-your-voice: When multimodal meets zero-shot low-light image enhancement (2024)
54. Zhang, X., Zhao, Y., Gu, C., Lu, C., Zhu, S.: Spa-former: An effective and lightweight transformer for image shadow removal. In: *2023 International Joint Conference on Neural Networks (IJCNN)*. pp. 1–8. IEEE (2023)
55. Zhang, Y., Guo, X., Ma, J., Liu, W., Zhang, J.: Beyond brightening low-light images. *International Journal of Computer Vision* **129**, 1013–1037 (2021)
56. Zhang, Y., Zhang, J., Guo, X.: Kindling the darkness: A practical low-light image enhancer. In: *Proceedings of the 27th ACM international conference on multimedia*. pp. 1632–1640 (2019)
57. Zhang, Z., Jiang, Y., Jiang, J., Wang, X., Luo, P., Gu, J.: Star: A structure-aware lightweight transformer for real-time image enhancement. In: *Proceedings of the IEEE/CVF International Conference on Computer Vision*. pp. 4106–4115 (2021)
58. Zhao, Q., Zhang, X., Tang, H., Gu, C., Zhu, S.: Enlighten-anything: When segment anything model meets low-light image enhancement. *arXiv preprint arXiv:2306.10286* (2023)
59. Zheng, Z., Wu, C.: U-shaped vision mamba for single image dehazing. *arXiv preprint arXiv:2402.04139* (2024)
60. Zhu, L., Liao, B., Zhang, Q., Wang, X., Liu, W., Wang, X.: Vision mamba: Efficient visual representation learning with bidirectional state space model. *arXiv preprint arXiv:2401.09417* (2024)